Exchange Interaction in Metal−Radical Systems: Chloro(*meso*-tetraphenylporphyrinato)chromium(III)'s and (Hexafluoroacetylacetonato)manganese(II) Ligated with 3- and 4-(*N*-Oxy-*N*-*tert*-butylamino)pyridines

Makoto Kitano, Yoichiro Ishimaru, Katsuya Inoue, Noboru Koga, and Hiizu Iwamura*

Department of Chemistry, Graduate School of Science, The University of Tokyo, 7-3-1 Hongo, Bunkyo-ku, Tokyo 113, Japan

Received June 3, 1994[⊗]

Ligands 3- and 4-(*N*-oxy-*N*-*tert*-butylamino)pyridines (3NOPy and 4NOPy, respectively) bearing unpaired electrons were prepared and allowed to react with chloro(*meso*-tetraphenyl- and *meso*-tetrakis(*p*-methoxyphenyl)-porphyrinato)chromium(III)'s {Cr(TPP)Cl and Cr(TAP)Cl, respectively} and (hexafluoroacetylacetonato)-manganese(II) {Mn(hfac)$_2$} to give the complexes Cr(TPP)(3- and 4NOPy)Cl, Cr(TAP)(3- and 4NOPy)Cl, Mn(3- and 4NOPy)$_2$(hfac)$_2$, and [Mn(4NOPy)(hfac)$_2$]$_n$ (n = 2 for complex **a** and n > 2 for **b**). The complex Mn-(4NOPy)$_2$(hfac)$_2$ crystallizes in the triclinic space group $P\bar{1}$, with a = 11.592(2) Å, b = 12.826(2) Å, c = 6.5853-(2) Å, α = 98.20(1)°, β = 92.28(1)°, γ = 64.01(1)°, and Z = 1, and has two 4NOPy's coordinated with the manganese ion not at the nitroxide radical but at the pyridine nitrogens in a *trans* configuration. The complex **a**, [Mn(4NOPy)(hfac)$_2$]$_2$, monoclinic space group $P2_1/n$ with a = 9.324(3) Å, b = 20.055(4) Å, c = 13.763(3) Å, β = 100.10(2)°, and Z = 4, has a cyclic dimer structure in which either manganese ion is coordinated with the pyridine nitrogen of one ligand 4NOPy and the oxygen atom of the nitroxide of the other ligand in a *cis* configuration. EPR spectroscopy, SQUID susceptometry, and Faraday-balance magnetometry revealed that the chromium ions in Cr(TPP)(3- and 4NOPy)Cl and Cr(TAP)(3- and 4NOPy)Cl interact ferro- and antiferromagnetically with the unpaired electrons of 3- and 4NOPy to produce quintet and triplet ground states, respectively. In Mn(4NOPy)$_2$(hfac)$_2$, the exchange coupling parameter J/k_B between the S = $^5/_2$ manganese(II) ion and the S = $^1/_2$ nitroxide radicals has been estimated to be −12.4 ± 0.1 K by fitting a linear three-spin model to the observed μ_{eff} vs T plot. In Mn(3NOPy)$_2$(hfac)$_2$, the μ_{eff} value of 5.74 μ_B at 290 K was rather insensitive to temperature. The manganese ions in 1:1 complex **a** interact with the directly attached nitroxide radical strongly in an antiferromagnetic fashion and the effective exchange coupling between the two residual spins S = $^4/_2$ has been evaluated to be ferromagnetic. The μ_{eff} value for the complex **b** surpassed a theoretical value of 8.94 μ_B for the dimer with S = $^4/_2$ at 16 K, suggesting a linear chain structure for complex **b**.

Introduction

Macroscopic spins in polymeric metal complexes consisting of transition metals M and ligands L carrying organic free radicals R are of great interest to scientists aiming at construction of molecular based magnetic materials.[1] One of the highlights in these metal−radical systems is the oligomers/polymers of (hexafluoroacetylacetonato)manganese and copper/nitronyl nitroxide complexes prepared and studied extensively by Gatteschi and co-workers.[2] In these and other related cases,[3] however, the radical centers also serve as the ligating centers (L = R) and it is difficult to control the sign of the often antiferromagnetic exchange coupling between the spins of the metals and the organic radicals. Our alternative strategy is based on the idea that, when transition metals are coordinated with certain π-conjugated bis(monodentate) ligands, L−R−L, carrying π-radical centers (R) remote from the ligating centers (L) as depicted in formula **1**, the sign of the magnetic interaction between the spin centers might be controlled by a through-ligand interaction.

1

In this linear chain (**1**), our target system, there are three types of magnetic interaction of fundamental importance, M and R in M−L−R, M and two R's in R−L−M−L−R, and R and two M's in M−L−R−L−M. As a step nearer to full understanding of spin system **1**, we have investigated, in this paper, some prototypes of these interactions in which 3- and 4-(*N*-oxy-*N*-*tert*-butylamino)pyridines, 3NOPy and 4NOPy, were employed as ligands L−R.

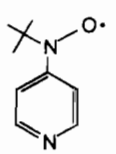

4NOPy

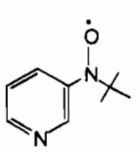

3NOPy

[⊗] Abstract published in *Advance ACS Abstracts,* November 15, 1994.

(1) *Magnetic Molecular Materials*; Gatteschi, D., Kahn, O., Miller, J. S., Palacio, F., Eds.; NATO ASI Series E; Kluwer: Dordrecht, The Netherlands, 1991; Vol. 198.
(2) Caneschi, A.; Chiesi, P.; David, L.; Ferraro, F.; Gatteschi, D.; Sessoli, R. *Inorg. Chem.* **1993**, *32*, 1445. Caneschi, A.; Gatteschi, D.; Rey, P. *Prog. Inorg. Chem.* **1991**, *39*, 331. Caneschi, A.; Gatteschi, D.; Renard, J. P.; Rey, P.; Sessoli, R., *Inorg. Chem.* **1989**, *28*, 1976. Caneschi, A.; Gatteschi, D.; Laugier, J.; Rey, P.; Sessoli, R. *Inorg. Chem.* **1988**, *27*, 1553.

0020-1669/94/1333-6012$04.50/0

(A) Metal−Radical Interaction in M−L−R. As a first step, it is important to know if the sign and magnitude of the magnetic interactions between transition metal M and organic radical center R could be predicted and controlled by the choice of L. More specifically, the question must be answered as to whether the spin polarization mechanism[4] widely used in purely organic high-spin systems can be applied to the regiospecificity of L in these metal−radical systems. For this purpose, we have chosen chlorochromium(III) porphyrins, Cr(TPP)Cl and Cr(TAP)Cl, ligated with 3NOPy and 4NOPy, and investigated by means of EPR spectroscopy and SQUID susceptometry the magnetic interaction between the spins of the Cr(III) and *tert*-butyl nitroxide radical contained in the sixth axial pyridine ligand.[5]

(B) Three-Center Interaction between M and Two R's in R−L−M−L−R. For this system,[6] (hexafluoroacetylacetonato)manganese(II), $Mn(hfac)_2$, was employed in place of Cr(TPP)Cl or Cr(TAP)Cl, since, contrary to air-sensitive Cr^{II}(TPP) complexes,[7] octahedral Mn(II) complexes are quite stable. The three-center magnetic interaction in a system NOPy−manganese−NOPy of $Mn(NOPy)_2(hfac)_2$ was investigated by means of SQUID susceptometry.

(C) Cyclic Interaction between M and R in $[-M-L-R-]_n$. Additionally, two kinds of 1:1 complexes, $[Mn(4NOPy)(hfac)_2]_n$, were prepared and their magnetic properties were investigated. A cyclic array of four kinds of spins in the form **2** ($n = 2$) was confirmed at least in one of the complexes.

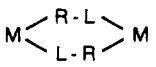

2

Experimental Section

General Methods. Infrared spectra were recorded on a Hitachi I-5040 FT-IR spectrometer. ^1H NMR spectra were measured on a JEOL 270 Fourier transform spectrometer using $CDCl_3$ as solvent and referenced to TMS. UV-visible absorption spectra were measured on a JASCO UVDEC-610C and Hitachi U-3300 spectrometer. High resolution mass spectra (HRMS) were record on a JEOL Datum JMS-SX102 spectrometer. Melting points were obtained with a MEL-TEMP heating block and uncorrected. Elemental analyses were performed in the Analytical Center of this Department.

Determination of the Binding Constants of (Porphyrinato)chromium(III)−NOPy Complexes. Titration of CrTPP (initial concentration of ca. 1 mM) with 3- or 4NOPy in CH_2Cl_2 was monitored using absorptions at 611.2 nm {ϵ (complex) = 1.3×10^4} characteristic of the coordination of CrTPP with a pyridyl nitrogen at the apical position. Binding constants (log K) of 4.0 and 4.4 were obtained for 3NOPy and 4NOPy, respectively, using a standard method.[8] The former value is in good agreement with that (4.1) for parent ligand pyridine in the literature.[8a] The higher value for ligand 4NOPy indicates the higher Lewis basicity and is ascribed to the electron-donating effect of the nitroxide radical as a substituent in conjugation with the pyridine nitrogen.

(3) Inoue, K.; Iwamura, H. *J. Am Chem Soc.* **1994**, *116*, 3173. Caneschi, A.; Dei, A.; Gatteschi, D., *J. Chem. Soc.,Chem. Commun.* **1992**, 630. Burdukov, A. B.; Ovcharenko, V. I.; Ikorski, V. N.; Pervukhina, N. V.; Podberezskaya, N. V.; Grigor'ev, I. A.; Larionov, S. V.; Volodarsky, L. B. *Inorg. Chem.* **1991**, *30*, 972. Eaton, G. R.; Eaton, S. S. *Acc. Chem. Res.* **1988**, *21*, 107.
(4) Iwamura, H. *Adv. Phys. Org. Chem.* **1990**, *26*, 179. Dougherty, D. A. *Acc. Chem. Res.* **1990**, *24*, 88.
(5) Kitano, M.; Koga, N.; Iwamura, H. *J. Chem. Soc., Chem. Commun.* **1994**. 447.
(6) Caneschi, A.; Ferraro, F.; Gatteschi, K.; Rey, P.; Sessoli, R. *Inorg. Chem.* **1990**, *29*, 4217.
(7) Scheidt, W. R.; Brinegar, A. C.; Kirner, J. F.; Reed, C. A. *Inorg. Chem.* **1979**, *18*, 3610. Reed, C. A.; Kouba, J. K.; Grimes, C. J.; Cheung, S. K. *Inorg. Chem.* **1978**, *17*, 2666.
(8) (a) Summerville, D. A.; Jones, R. D.; Hoffman, B. M.; Basolo, F. *J. Am. Chem. Soc.* **1977**, *99*, 8195. (b) Bernardo, A. R.; Stoddart, J. F.; Kaifer, A. E. *J. Am. Chem. Soc.* **1992**, *114*, 10264.

Table 1. Crystallographic Data for $Mn(4NOPy)_2(hfac)_2$ and $[Mn(4NOPy)(hfac)_2]_2$

	$Mn(4NOPy)_2(hfac)_2$	$[Mn(4NOPy)(hfac)_2]_2$ (complex **a**)
chem formula	$C_{28}H_{28}N_4O_6F_{12}Mn$	$C_{38}H_{30}N_4O_{10}F_{24}Mn_2$
a, Å	11.592(2)	9.324(3)
b, Å	12.826(2)	20.055(4)
c, Å	6.5853(2)	13.763(3)
α, deg	98.20(1)	
β, deg	92.28(1)	100.10(2)
γ, deg	64.91(1)	
V, Å^3	877.3(3)	2534(1)
Z	1	4
fw	799.47	1268.521
space group	$P\bar{1}$ (No. 2)	$P2_1/n$ (No. 14)
T, °C	23.0	22
λ, Å	0.710 69	0.710 69
ϱ_{calc}, g cm^{-3}	1.513	1.663
μ, cm^{-1}	4.84	6.17
$R(F_o)^a$	0.061	0.087
$R_w(F_o)^a$	0.052	0.080

^{a} $R = \sum||F_o| - |F_c||/\sum|F_o|$; $R_w = [(\sum w(|F_o| - |F_c|)^2/\sum wF_o^2)]^{1/2}$.

Table 2. Positional Parameters and Temperature Factors (Å^2 × 10^3) for $Mn(4NOPy)_2(hfac)_2$[a]

atom	x	y	z	B(eq)
Mn(1)	0	0	0	3.50(2)
F(6)	0.2498(3)	0.2349(2)	−0.2652(4)	8.9(1)
F(7)	0.0531(3)	0.3267(2)	−0.1892(5)	10.0(1)
F(8)	0.1136(3)	0.2027(2)	−0.4544(4)	7.73(8)
F(9)	−0.3457(3)	0.0405(3)	−0.4474(4)	9.5(1)
F(10)	−0.4239(3)	−0.0443(3)	−0.2955(5)	11.8(1)
F(11)	−0.4538(3)	0.1243(3)	−0.1862(5)	14.6(1)
O(11)	0.0518(2)	0.1072(2)	−0.1641(3)	3.91(6)
O(13)	−0.3198(4)	0.4243(3)	0.8467(4)	9.8(1)
O(14)	−0.1758(2)	0.0279(2)	−0.1601(3)	4.02(6)
N(11)	−0.2964(3)	0.4491(3)	0.6773(5)	5.7(1)
N(12)	−0.1104(3)	0.1580(2)	0.2314(4)	4.04(7)
C(16)	−0.2371(3)	0.3543(3)	0.5218(5)	4.3(1)
C(17)	−0.2091(3)	0.2439(3)	0.5640(5)	4.2(1)
C(18)	0.1424(4)	0.2246(4)	−0.2604(7)	5.3(1)
C(19)	−0.1401(4)	0.2663(4)	0.1914(6)	5.4(1)
C(20)	−0.3287(5)	0.5754(4)	0.6655(7)	6.4(1)
C(21)	−0.2013(4)	0.3649(3)	0.3280(6)	5.7(1)
C(22)	−0.3708(4)	0.0276(5)	−0.2649(7)	5.7(1)
C(24)	−0.4159(5)	0.6151(4)	0.4857(8)	8.8(2)
C(25)	−0.2051(6)	0.5889(5)	0.6468(9)	10.2(2)
C(26)	−0.4006(8)	0.6448(5)	0.8621(9)	14.8(2)
C(27)	0.1449(3)	0.1319(3)	−0.1345(5)	3.52(8)
C(28)	0.2450(3)	0.0915(3)	−0.0008(5)	4.1(1)
C(30)	−0.2514(3)	−0.0141(3)	−0.1317(5)	3.53(8)
C(31)	−0.1464(3)	0.1497(3)	0.4176(5)	4.2(1)

[a] Standard deviations in the last significant digits are given in parentheses. $B_{eq} = 8/3\pi^2(U_{11}(aa^*)^2 + U_{22}(bb^*)^2 + U_{33}(cc^*)^2 + 2U_{12}aa^*bb^* \cos\gamma + 2U_{13}aa^*cc^* \cos\beta + 2U_{23}bb^*cc^* \cos\alpha)$.

X-ray Crystal and Molecular Structure Analyses. All the X-ray data were collected using Mo Kα radiation on a Rigaku AFC5R or AFC7R four circle diffractometer. Pertinent crystallographic parameters and refinement data are listed in Table 1. The structures were solved in $P\bar{1}$ and $P2_1/n$ for $Mn(4NOPy)_2(hfac)_2$ and complex **a**, $[Mn(4NOPy)(hfac)_2]_2$, respectively, by direct methods and refinement converged using the full-matrix least squares of the TEXAN Ver. 2.0 program (Molecular Structure Corp.). All non-hydrogen atoms were refined anisotropically; hydrogen atoms were included at standard positions (C−H 0.96 Å, C−C−H 109.5, 120, or 180°) and refined isotropically using a rigid model. Final atomic coordinates and isotropic thermal factors are reported in Tables 2 and 3 for $Mn(4NOPy)_2(hfac)_2$ and $[Mn(4NOPy)(hfac)_2]_2$, respectively.

EPR Spectra and Magnetic Measurements. EPR spectra were obtained on a Bruker ESP 300 X band spectrometer equipped with an Air Products LTD-3-110 liquid helium transfer system. The measuring temperature was regulated by a Scientific Instrument Inc. series 5500 temperature controller. Sample solutions in quartz EPR cells (5 mm × 200 mm) were degassed by four freeze−thaw cycles and sealed.

Table 3. Positional Parameters and Temperature Factors (Å² × 10³) for [Mn(4NOPy)(hfac)₂]₂ (Complex **a**)[a]

atom	*x*	*y*	*z*	*B*(eq)
Mn(1)	0.1469(2)	0.04507(8)	0.3028(1)	3.33(7)
F(1)	0.068(1)	0.2151(5)	0.0662(7)	13.3(7)
F(2)	0.101(2)	0.2859(5)	0.1673(8)	16.4(8)
F(3)	−0.102(1)	0.2544(7)	0.1153(9)	17.1(8)
F(4)	0.036(2)	0.2518(6)	0.511(1)	19(1)
F(5)	−0.119(1)	0.186(1)	0.511(1)	22(1)
F(6)	0.074(2)	0.1692(8)	0.5669(8)	21(1)
F(7)	−0.313(1)	−0.0516(6)	0.160(1)	17(1)
F(8)	−0.239(1)	−0.1205(8)	0.247(1)	20(1)
F(9)	−0.238(1)	−0.1304(8)	0.104(1)	20(1)
F(10)	0.341(2)	−0.0452(7)	0.039(1)	18(1)
F(11)	0.381(1)	−0.1111(8)	0.122(1)	18(1)
F(12)	0.215(1)	−0.113(1)	0.000(1)	27(1)
O(1)	0.3395(7)	0.1093(3)	0.3399(5)	3.8(3)
O(2)	−0.0431(8)	−0.0157(4)	0.2585(5)	4.5(4)
O(3)	0.2345(8)	−0.0123(4)	0.1981(5)	4.5(4)
O(4)	0.0474(7)	0.1023(4)	0.4024(5)	3.9(4)
O(5)	0.0618(7)	0.1254(4)	0.2007(5)	4.2(4)
N(1)	0.4731(9)	0.1043(5)	0.3255(6)	3.9(4)
N(2)	0.2539(8)	−0.0189(4)	0.4307(6)	3.4(4)
C(1)	−0.207(2)	−0.093(1)	0.177(1)	8(1)
C(2)	−0.059(1)	−0.0581(6)	0.193(1)	5.5(7)
C(3)	0.033(2)	−0.0815(7)	0.131(1)	7.0(8)
C(4)	0.173(1)	−0.0545(7)	0.1391(9)	5.3(7)
C(5)	0.265(2)	−0.107(2)	0.081(1)	21(2)
C(6)	0.513(1)	0.1440(7)	0.2415(8)	5.1(6)
C(7)	0.428(1)	−0.0772(5)	0.5913(7)	3.2(5)
C(8)	0.454(1)	−0.0887(5)	0.4983(8)	3.5(5)
C(9)	0.313(1)	−0.0357(7)	0.6041(8)	4.7(6)
C(10)	0.366(1)	−0.0604(5)	0.4188(7)	3.4(5)
C(11)	0.229(1)	−0.0094(6)	0.5212(8)	4.0(5)
C(12)	0.473(2)	0.2161(8)	0.265(1)	12(1)
C(13)	0.423(2)	0.1218(8)	0.148(1)	10(1)
C(14)	0.671(2)	0.141(1)	0.237(1)	14(1)
C(15)	−0.004(2)	0.194(1)	0.488(1)	9(1)
C(16)	0.028(1)	0.1642(6)	0.3985(8)	4.1(6)
C(17)	0.027(1)	0.2068(6)	0.322(1)	5.2(6)
C(18)	0.042(1)	0.1836(6)	0.227(1)	4.3(6)
C(19)	0.027(2)	0.2337(8)	0.145(1)	6.8(8)

[a] Standard deviations in the last significant digits are given in parentheses. $B_{eq} = 8/3\pi^2(U_{11}(aa^*)^2 + U_{22}(bb^*)^2 + U_{33}(cc^*)^2 + 2U_{12}aa^*bb^* \cos\gamma + 2U_{13}aa^*cc^* \cos\beta + 2U_{23}bb^*cc^* \cos\alpha)$.

Magnetic susceptibilities and magnetizations were measured on a Quantum Design MPMS$_2$ SQUID susceptometer and an Oxford Faraday magnetic balance, respectively. Data were corrected for the magnetization of the sample holder and cell and for diamagnetic contributions which were estimated from Pascal's constants.

Preparation of Ligands and the Cr and Mn Complexes. Unless otherwise stated, the preparative reactions were carried out under a high purity dry nitrogen atmosphere. Diethyl ether and toluene were distilled from sodium benzophenone ketyl. 2-Methyl-2-nitrosopropane,[9] chloro(*meso*-tetraphenyl- and *meso*-tetrakis(*p*-methoxyphenyl)porphyrinato)chromium(III)'s, Cr(TPP)Cl and Cr(TAP)Cl,[8a] respectively, were prepared and purified by procedures reported in the literature. (Hexafluoroacetylacetonato)manganese, Mn(hfac)$_2$·2H$_2$O, and acetylacetonatomanganese, Mn(acac)$_2$•2H$_2$O, were prepared according to the literature.[10,11]

Organic radicals 3- and 4NOPy are reported in the literature only as spin adducts of a spin trapping experiment[12] and have not been obtained authentically. They have now been prepared and purified by a procedure employed for analogous phenyl derivatives.[13] Namely, lithiation of the corresponding bromopyridine followed by reaction with 2-nitroso-2-methylpropane gave the hydroxyamines which were then treated with freshly prepared Ag_2O in CH_2Cl_2 to give the nitroxide radicals. They were found to be stable in solution under nitrogen atmosphere for several weeks while unstable in the solid state. They were used for spectral and magnetic measurements immediately after preparation. EPR spectra of the nitroxide radicals in $CHCl_3$ showed well-separated characteristic signals which were simulated to give the hyperfine splitting constants (hfs) that are in good agreement with those in the literature.[12]

The chromium(III)−NOPy complexes were obtained from solutions containing NOPy in slight excess.

3-(*N-tert*-Butyl-*N*-hydroxyamino)pyridine (3NOHPy). To a solution of 10 g (63 mmol) of 3-bromopyridine in 300 mL of ether were added 40 mL of a 1.6 M solution of *n*-butyllithium in *n*-hexane at −78 °C. After stirring for 30 min, a solution of 5.5 g (63 mmol) of 2-methyl-2-nitrosopropane in 60 mL of ether was added dropwise. The reaction mixture was stirred for one hour at −78 °C and then left overnight at room temperature. After the usual workup, a brown solid was chromatographed on aluminum oxide with $CHCl_3$ as eluent to give 4.8 g (46% yield) of the hydroxyamine as a white solid: mp 112−115 °C, ^{1}H NMR (270 MHz, $CDCl_3$) δ 1.13 (9H, s), 6.54 (1H, br. s), 7.19 (1H, dd, J = 8.79 and 4.76 Hz), 7.62 (1H, m), 8.31 (1H, dd, J = 4.76 and 1.47 Hz), 8.43 (1H, d, J = 2.2 Hz). Anal. Calcd for $C_9H_{14}ON_2$: C, 65.03; H, 8.49; N, 16.85. Found: C, 64.92; H, 8.44; N, 16.59.

4-(*N-tert*-Butyl-*N*-hydroxyamino)pyridine (4NOHPy). This was prepared using 4-bromopyridine in place of 3-bromopyridine in a manner similar to the preparation of the 3-hydroxyamine derivative. Chromatography on aluminum oxide with $CHCl_3$ as eluent gave 4-hydroxyaminopyridine (29% yield) as a white solid: mp 172−175 °C (decomp.), ^{1}H NMR (270 MHz, $CDCl_3$) δ 1.22 (9H, s) 7.15 (2H, d, J = 6.23 Hz), 8.41 (2H, d, J = 6.23 Hz). HRMS, *m/z*: found, 166.1125 (21.4 %); calcd for $C_9H_{14}ON_2$, 166.1106.

3-(*N-tert*-Butyl-*N*-oxyamino)pyridine (3NOPy). Freshly prepared silver oxide (1.0 g) was suspended in a solution of 0.3 g (1.8 mmol) of 3NOHPy in 150 mL of CH_2Cl_2 for 30 min. The whole mixture was dried on anhydrous magnesium sulfate and filtrated. The filtrate was condensed when necessary and used for the preparation of the chromium porphyrin complex without isolation. UV−vis (CH_2Cl_2): 290, 380, 490 (sh) nm. EPR ($CHCl_3$): g = 2.0060, a_N = 12.6 (nitroxide N), 0.97 (pyridine N) and a_H = 1.63 (2-, 4- and 6-H), 0.87 (5-H) G.

4-(*N-tert*-Butyl-*N*-oxyamino)pyridine (4NOPy). This was prepared using 4NOHPy in place of 3NOHPy in a manner similar to 3NOPy. UV-vis (CH_2Cl_2): 295, 372, 519 nm. EPR ($CHCl_3$): a_N = 11.0 (nitroxide N), 2.1 (pyridine N) and a_H = 1.35 (3- and 5-H), 0.61 (2- and 6-H) G.

(Porphyrinato)chromium(III)−Pyridyl Nitroxide Radical Complexes, Cr(TPP)(3- and 4NOPy)Cl and Cr(TAP)(3- and 4NOPy)Cl. These were precipitated by addition of *n*-hexane to mixtures of the chlorochromium(III) porphyrins and a slight excess of the corresponding NOPy in CH_2Cl_2. The precipitates were washed with *n*-hexane to remove excess nitroxide radicals, and then dried under reduced pressure to give dark green powders.

A concentrated solution (> 10 mM) of the dark green powder sample of Cr(TPP)(4NOPy)Cl in CH_2Cl_2 showed an absorption maximum at 611 nm charactristic of a Cr^{III}(TPP) complex with an axial pyridine ligand. The λ_{max} was at 617 nm for the Cr(TAP)(3- and 4NOPy)Cl complexes. EPR spectra of dilute solutions (<0.1 mM) of the dark green powder samples showed three-line signals characteristic of dissociated free nitroxides. Cr(TPP)(3NOPy)Cl gave a satisfactory analytical result. On the basis of the chlorine contents, the other three seemed to contain some residual solvent CH_2Cl_2; satisfactory elemental analysis could not be obtained for Cr(TAP)(3- and 4NOPy)Cl. Cr(TPP)(3NOPy)Cl. Anal. Calcd for $C_{53}H_{41}N_6OClCr$: C, 73.56; H, 4.78; N, 9.71; Cl, 4.10. Found : C, 73.27; H, 4.85; N, 9.94; Cl, 4.00. Cr(TPP)(4NOPy)Cl. Anal. Calcd for $C_{53}H_{41}N_6OClCr0.14CH_2Cl_2$: C, 72.78; H, 4.75; N, 9.59; Cl, 5.21. Found: C, 72.35; H, 4.79; N, 10.31; Cl, 5.28.

Bis{4-(*N-tert*-butyl-*N*-oxyamino)pyridine}(hexafluoroacetylacetonato)manganese(II) {Mn(4NOPy)$_2$(hfac)$_2$}. A solution of 0.3 g of (hexafluoroacetylacetonato)manganese(II) dihydrate in 60 mL of *n*-heptane was heated, and about 10 mL of the solvent was removed by azeotropic distillation. The solution was cooled down to room temperature, and a solution of 4NOPy (12 mM) in 100 mL of CH_2Cl_2

(9) Stowell, J. C. *J. Org. Chem.* **1971**, *36*, 3055.
(10) Cotton, F. A.; Holm, R. H. *J. Am. Chem. Soc.* **1960**, *82*, 2979.
(11) Charles, R. G. *Inorg. Synth.* **1960**, *6*, 164.
(12) Bentley, T. W.; John, J. A.; Johnstone, R. A. W. *J. Chem. Soc. Perkin II* **1973**, 1039.
(13) Kanno, F.; Inoue, K.; Koga, N.; Iwamura, H. *J. Phys. Chem.* **1993**, *97*, 13267. Kanno, F.; Inoue, K.; Koga, N.; Iwamura, H. *J. Am Chem. Soc.* **1993**, *115*, 847.

was added. The resulting mixture was dried on anhydrous sodium sulfate, filtered, reduced to ca. 60 mL on a rotary evaporator, and left overnight. The resulting brown precipitates were removed by filtration and the solution was left further. Dark brown bricklike crystals were obtained (30 mg). Anal. Calcd for $C_{28}H_{28}N_4O_6F_{12}Mn$: C, 42.07; H, 3.53; N, 7.01. Found: C, 42.10; H, 3.42; N, 7.26.

Bis{3-(*N*-*tert*-butyl-*N*-oxyamino)pyridine}(hexafluoroacetylacetonato)manganese(II) {Mn(3NOPy)$_2$(hfac)$_2$}. This was prepared in a similar manner to Mn(4NOPy)$_2$(hfac)$_2$ using 3NOPy in place of 4NOPy. Orange microcrystals were obtained. Anal. Calcd for $C_{28}H_{28}N_4O_6F_{12}Mn$: C, 42.07; H, 3.53; N, 7.01. Found: C, 41.82; H, 3.41; N, 7.28.

Bis{4-(*N*-*tert*-butyl-*N*-oxyamino)pyridine}(acetylacetonato)manganese(II){Mn(4NOPy)$_2$(acac)$_2$}. This was prepared in a similar manner to Mn(4NOPy)$_2$(hfac)$_2$ using Mn(acac)$_2$ in place of Mn(hfac)$_2$. Orange microcrystals were obtained. Anal. Calcd for $C_{28}H_{40}N_4O_6Mn$: C, 57.63; H, 6.91; N, 9.60. Found: C, 57.38; H, 6.78; N, 9.72.

(4-(*N*-*tert*-Butyl-*N*-oxyamino)pyridine)(hexafluoroacetylacetonato)manganese(II) {[Mn(4NOPy)(hfac)$_2$]$_n$} (1:1 Complexes a and b). These were prepared in a manner similar to Mn(4NOPy)$_2$(hfac)$_2$ using a 1:1 mixture of Mn(hfac)$_2$ and 4NOPy. Slow crystallization (1 week) and rapid precipitation (12 h) from the mixed solution gave 1:1 complexes **a** and **b**, respectively. Complex **a**, black needles: UV−vis (KBr) 361, 455, and 588 (sh) nm. Anal. Calcd for $C_{19}H_{15}N_2O_5F_{12}Mn$: C, 35.98; H, 2.38; N, 4.42. Found: C, 35.87; H, 2.43; N, 4.55. Complex **b**, black fine needle: UV−vis (KBr) 361, 449, and 600 (sh) nm. Anal. Calcd for $C_{19}H_{15}N_2O_5F_{12}Mn$: C, 35.98; H, 2.38; N, 4.42. Found: C, 35.69; H, 2.41; N, 4.40.

Results and Discussion

A. (Porphyrinato)chromium(III) Complexes with 3NOPy and 4NOPy. A-1. EPR Spectra of Cr(TPP)(NOPy)Cl and Cr(TAP)(NOPy)Cl. EPR spectra of toluene solutions of Cr(TPP)Cl in the presence of a slight excess of 3- and 4NOPy frozen at 10 K are shown in Figure 1. Other than signals at $g = 2$ due to the free nitroxide radicals present in excess; these spectra are characteristically different from each other and also quite different from those of Cr(TPP)Cl ligated with pyridine itself and 3- or 4-(*N*-*tert*-butyl-*N*-hydroxyamino)pyridines under similar conditions, indicating that magnetic interaction between the chromium(III) and the nitroxide radicals by coordination through the pyridyl nitrogen of NOPy is significant. As the temperature was raised from 10 to 115 K, the EPR signal intensities of Cr(TPP)(3NOPy)Cl decreased in accordance with Curie law, while new signals at 259, 279, 376, and 421 mT appeared at ca. 75 K at the expense of the decreasing signals in Cr(TPP)(4NOPy)Cl. The intensity of the new signals continued to increase with increasing temperature as shown by the spectrum at 115 K in Figure 1b′. Their resonance field positions are close to those observed in Cr(TPP)(3NOPy)Cl. As the temperature was increased further, both spectral shapes became similar to each other except for the signal at 157 mT for Cr(TPP)(4NOPy)Cl. The observed thermal behavior of the EPR spectra was reversible and reproducible, suggesting that quintet and triplet ground states might be produced by ferro- and antiferromagnetic interaction between Cr(III) ($S = {}^3/_2$) as the central metal of Cr(TPP)Cl and the nitroxide radical ($S = {}^1/_2$) on the sixth ligand in 3- and 4NOPy, respectively. New signals observed for Cr(TPP)(4NOPy)Cl above 75 K were assigned to thermally populated quintet species. From the temperature of 75 K, the energy difference ($\Delta E_{Q-T} = 4J$) between the quintet and triplet states was estimated to be greater than 630 J/mol. There was no significant difference in the overall EPR spectral behavior under similar conditions when Cr(TAP)Cl's were used (may be seen in Figure S2 of suplementary material) in place of Cr(TPP)Cl's.

A-2. Magnetic Susceptibility Measurements. To understand the magnetic interaction between chloro(porphyrinato)chromium(III) and two isomeric nitroxide radicals on the ligated pyridines in more detail, magnetic susceptibilities of the powder samples were measured in the temperature range 5−300 K at a constant magnetic field of 0.2 T. The temperature dependence of the effective magnetic moment (μ_{eff}) of Cr(TPP)(3- and 4NOPy)Cl together with Cr(TPP)(Py)Cl as a reference is shown in Figure 2.

The μ_{eff} values at 300 K were 3.95 and 3.41 μ_B for Cr(TPP)(3- and 4NOPy)Cl, respectively. As the temperature was decreased, the μ_{eff} value for Cr(TPP)(3NOPy)Cl gradually increased between 300 and 24 K and reached a maximum of $\mu_{eff} = 4.34\ \mu_B$ at 24 K, while that of Cr(TPP)(4NOPy)Cl decreased monotonically from 300 to 70 K and became nearly constant at 70 to 13 K. The μ_{eff} values for Cr(TPP)(Py)Cl were almost constant in all the temperature range studied. Sharp decreases of the μ_{eff} values below 24 and 13 K for Cr(TPP)(3- and 4NOPy)Cl, respectively, suggest the presence of intermolecular antiferromagnetic interaction.

The observed temperature dependencies of the μ_{eff} values for Cr(TPP)(3- and 4NOPy)Cl were analyzed in terms of a model in which quintet and triplet states in equilibrium are separated by $4J$. The intermolecular interaction was taken into account by a Weiss field. Fitting of eq 1 to the observed values was

$$\mu_{eff}/\mu_B = \sqrt{\frac{3g^2T}{(T-\theta)}\frac{2+10\exp\{-(-4J)/k_BT\}}{3+5\exp\{-(-4J)/k_BT\}}} \quad (1)$$

refined by means of a least-squares method, where all the symbols have their usual meaning. From the best fitted theoretical curves, parameters J/k_B ($\Delta E_{T-Q} = 4J$), θ, and g were evaluated to be 12.3 ± 0.3 K, −3.4 K, and 1.93 for Cr(TPP)(3NOPy)Cl and −77 ± 0.8 K, −1.1 K, and 1.89 for Cr(TPP)(4NOPy)Cl, respectively. Isomeric Cr(TAP)(NOPy)Cl's showed similar temperature dependence of μ_{eff} although intermolecular antiferromagnetic interactions at low temperature were somewhat weakened. Parameters J/k_B, θ, and g in eq 1 were found to be 16 ± 0.3 K, −0.3 K, and 1.82 for Cr(TAP)(3NOPy)Cl and −86 ± 1.5 K, −0.23 K, and 1.86 for Cr(TAP)(4NOPy)Cl, respectively (may be seen in Figure S1 of supplementary material).

The J values thus obtained for Cr(TPP)(3- and 4NOPy)Cl clearly show that the former has a quintet ground state and is a mixture of quintet and thermally populated triplet states in equilibrium in the temperature range 5−300 K, while the latter has a triplet ground state and a thermally accessible quintet state begins to contribute at temperatures above ca. 70 K. Although no signals due to the thermally populated triplet state were observed in the EPR spectra for Cr(TPP)(3NOPy)Cl,[14] the temperature dependency of that of Cr(TPP)(4NOPy)Cl was consistent with the results from the SQUID susceptibility measurement.

A comment should be made on the magnitude of the g values which ranges from 1.82 to 1.93 and is slightly lower than the typical values of 1.93−1.99 for hexacoordinated Cr(III) complexes.[8] There are at least two methods for the analysis of the temperature dependent behavior of μ_{eff} values according to eq 1. One assumes $g = 2$, while the other optimizes g as a parameter as well. In the latter case, any error in the concentration of the unpaired electrons due possibly to the sample purity, weighting the sample, and/or miscalibration of the susceptometer may be accumulated in the g value. Since the J values are of interest in this study, latter method of analysis has been adopted with the aim of attenuating the dispersion of them. As described in Experimental Section, the elemental analytical data suggested the samples of Cr(TPP)(4NOPy)Cl and Cr(TAP)(3- and 4NOPy)-

(14) Those signals were probably weak and were buried under strong quintet signals.

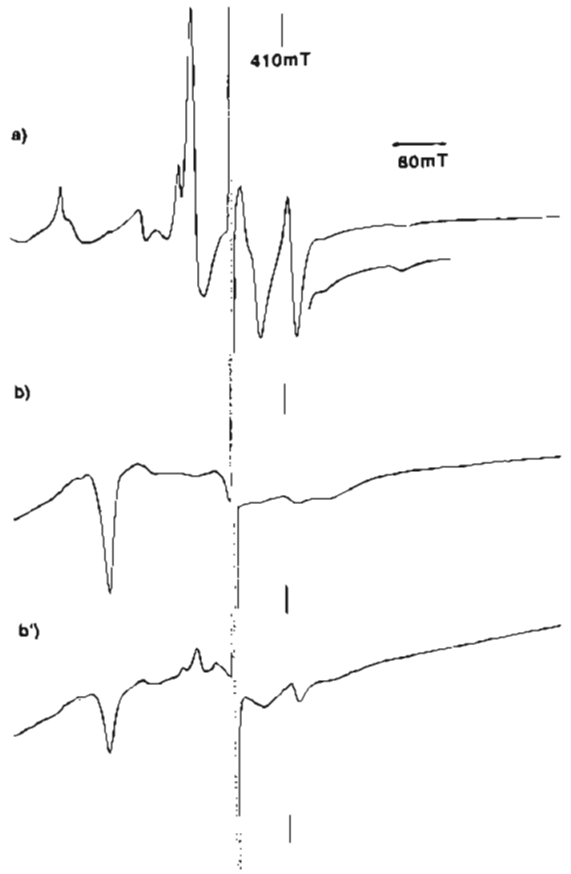

Figure 1. EPR spectra (ν = 9.392 GHz) in toluene matrices of (a) Cr(TPP)(3NOPy)Cl at 10 K and (b and b') Cr(TPP)(4NOPy)Cl at 10 and 115 K, respectively.

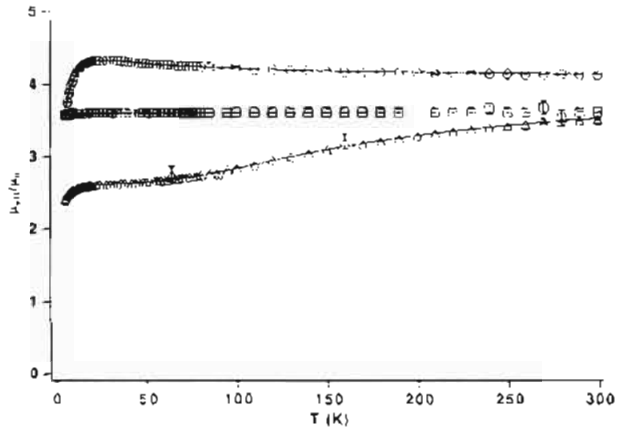

Figure 2. Temperature dependence of the effective magnetic moments μ_{eff} of Cr(TPP)(3NOPy)Cl (O) Cr(TPP)(4NOPy)Cl (△) and Cr(TPP)(Py)Cl (□). Solid curves are theoretical ones calculated on the basis of eq 1 with the optimized parameters given in text.

Cl are not free from solvent CH_2Cl_2. When these data are taken into account, the g values are evaluated to be 1.90, 1.83, and 1.89, respectively.

B. 1:2 $Mn^{II}(hfac)_2$ Complexes with 3NOPy and 4NOPy. B-1. X-ray Crystal and Molecular Structure of $Mn(4NOPy)_2(hfac)_2$. The manganese complexes are suggested by elemental analyses to be hexacoordinated with two hfac's and two pyridyl ligands. In principle there are two types of coordination, *cis* and *trans*, with respect to two NOPy's each of which has two ligating sites, the pyridyl nitrogen and the oxygen of the nitroxide radical. Fortunately, $Mn(4NOPy)_2(hfac)_2$ gave a dark bricklike crystals amenable to X-ray crystal structure analysis. It was not possible to grow crystals for the corresponding 3NOPy complex.

Table 4. Selected Bond Distances (Å) and Angles (deg) for $Mn(4NOPy)_2(hfac)_2$[a]

Bond Lengths (Å)			
Mn−O(14)	2.171(2)	O(13)−N(11)	1.272(3)
Mn−O(11)	2.143(3)	N(11)−C(16)	1.411(4)
Mn−N(12)	2.268(3)		
Bond Angles (deg)			
O(14)−Mn−N(12)	89.07(9)		83.96(8)
	90.93(9)	O(11)−Mn−N(12)	90.74(9)
O(14)−Mn−O(11)	96.93(8)		89.26(9)

[a] Standard deviations in the last significant digits are given in parentheses.

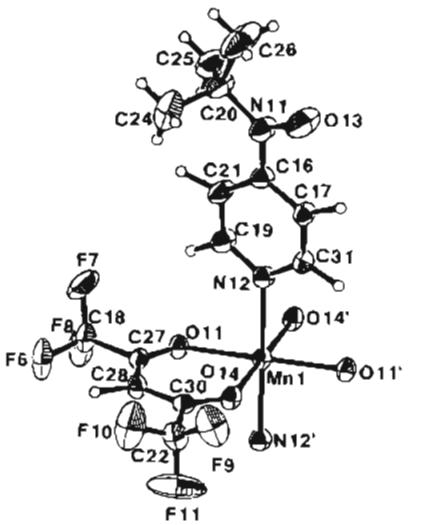

Figure 3. ORTEP drawing of about a half of the centrosymmetric structure of $Mn(4NOPy)_2(hfac)_2$ at 30% probability.

Crystallographic data and experimental parameters for $Mn(4NOPy)_2(hfac)_2$ are summarized in Table 1. Selected bond lengths and angles are given in Table 4. As shown in the partial ORTEP drawing in Figure 3, two pyridyl nitrogen atoms are ligated to a manganese(II) ion in the *trans* form. The bond distances of Mn−N and Mn−O are 2.27 and 2.16 Å, respectively, and the coordination geometry is an elongated distorted octahedron. The angle between the planes of the *tert*-butyl nitroxide moiety and the pyridine ring is only 1.7°, a value considerably smaller than phenyl *N-tert*-butyl nitroxides.[13] The observed near coplanarity suggests that the electron spin of the nitroxide radical center would be effectively delocalized onto the pyridine ring, corroborating the EPR result of the free ligands where the nitrogen hyperfine coupling with the nitroxide nitrogen is reduced from a typical value of 15 G to 11.0 G and that with the pyridyl nitrogen is meaningful (2.1 G) in 4NOPy; those in 3NOPy are greater for the nitroxide nitrogen (12.6 G) and smaller for the pyridine nitrogen (0.97 G).

In the crystal structure of $Mn(4NOPy)_2(hfac)_2$, the oxygen atom O(13) of a nitroxide radical is only 3.31 and 3.46 Å apart from carbons C(19) and C(21), respectively, of a pyridine ring belonging to the adjacent complex molecule. A possible intermolecular magnetic interaction due to these short distances will be taken into account by a Weiss field.

B-2. Magnetic Properties of $Mn(3NOPy)_2(hfac)_2$ and $Mn(4NOPy)_2(hfac)_2$. The magnetic susceptibilities for both the 1:2 complexes were measured in the temperature range 2−300 K at constant field of 100 mT. The effective magnetic moment values of $Mn(3NOPy)_2(hfac)_2$ and $Mn(4NOPy)_2(hfac)_2$ at 290 K were 5.74 and 6.35 μ_B, respectively. The latter value is slightly smaller than but nearly equal to the theoretical spin-only value $\{\mu_{eff} = g\sqrt{S(S+1)}\}$ of 6.40 for four degenerate states ($S = {}^3/_2, {}^5/_2, {}^5/_2$, and ${}^7/_2$) with $g = 2$.

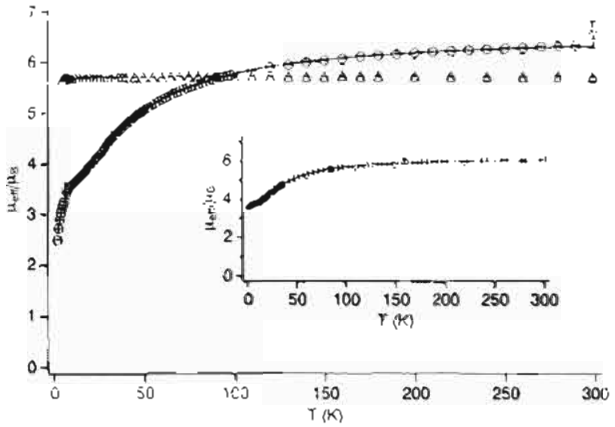

Figure 4. Temperature dependence of the effective magnetic moments μ_{eff} of $Mn(4NOPy)_2(hfac)_2$ (○) and $Mn(3NOPy)_2(hfac)_2$ (△). The inset shows a similar plot for $Mn(4NOPy)_2(acac)_2$. Solid curves are theoretical ones calculated on the basis of eq 2 with the optimized parameters given in text.

As the temperature was lowered, the μ_{eff} values of $Mn(4NOPy)_2(hfac)_2$ decreased gradually, reached an S-shaped plateau at ca. 20 K, and then decreased steeply below 10 K (Figure 4). The μ_{eff} value approaching 3.9 μ_B at ca. 10−20 K is qualitatively interpreted in terms of the spin-only value $\{\mu_{eff} = g\sqrt{S(S+1)}\}$ for $S = {}^3/_2$.

In order to analyze the temperature dependence of the observed μ_{eff} values for $Mn(4NOPy)_2(hfac)_2$ more quantitatively, a linear three-spin model suggested by the X-ray crystal and molecular structure was assumed. Its spin Hamiltonian is written as

$$H = -2J(S_1S_M + S_MS_2)$$

for which the eigenvalues are obtained as

$$E_1(S = {}^3/_2) = 7J$$

$$E_2(S = {}^5/_2) = 2J$$

$$E_3(S = {}^5/_2) = 0$$

$$E_4(S = {}^7/_2) = -5J$$

Temperature dependence of the effective magnetic moment, μ_{eff}/μ_B is then given by eq 2,where all the symbols have their usual

$$\mu_{eff}/\mu_B = \sqrt{\frac{g^2T}{4(T-\theta)}\,\frac{30\exp\mathbf{A} + 105\exp\mathbf{B} + 252\exp\mathbf{C} + 105}{2\exp\mathbf{A} + 3\exp\mathbf{B} + 4\exp\mathbf{C} + 3}} \quad (2)$$

$$\mathbf{A} = \frac{-7J}{k_BT} \quad \mathbf{B} = \frac{-2J}{k_BT} \quad \mathbf{C} = \frac{5J}{k_BT}$$

meaning. The Weiss constant θ contains the intermolecular interaction expected from the crystal packing of the complex in which the distance of the oxygen of the N−O and C at the 2-position of the pyridine ring in the nearest molecule is 3.310 Å. This equation was fitted to the experimental data by means of a least-squares method. The best-fit parameters were $J/k_B = -12.4 \pm 0.1$ K, $\theta = -2.58 \pm 0.05$ K, and $g = 2.059$. The theoretical curve is included in Figure 4.

Similarly, the magnetic susceptibility of $Mn(4NOPy)_2(acac)_2$ was measured and its J, θ, and g values were estimated to be -10.2 ± 0.05 K, -0.2 ± 0.01 K, and 1.949, respectively, by applying a symmetric three spin model (eq 2). Its μ_{eff} vs T plot and the corresponding theoretical curve are given as inset in Figure 4. While the change in the diamagnetic ligands does not appear to alter the sign and therefore the mechanism of the exchange interaction between the metal and 4NOPy, it reduces the strength of the antiferromagnetic coupling by ca. 20%. The reduction in the coupling may be ascribed to the weakening of the coordination bond between the metal and 4NOPy by increasing the metal acac bond through its higher basicity than that of hfac.

The temperature dependence of the effective magnetic moment of $Mn(3NOPy)_2(hfac)_2$ is quite different from that of the 4NOPy complex analyzed above. The μ_{eff}/μ_B value of 5.74 at 300 K is close to 5.7 for $MnPy_2(hfac)_2$ obtained under similar conditions, and remained constant in the temperature range 300−2 K as shown in Figure 4. Although a bit smaller than a theoretical μ_{eff} value of 5.92, it suggests $S = {}^5/_2$. It appears as if the two 3NOPy ligands did not carry unpaired electrons. One of the reasonable explanations for the cancellation of the spins between two 3NOPy's occurred to us from a recent crystal and molecular structural study of the corresponding $Cu(hfac)_2(3NOPy)_2$ complex which showed similar μ_{eff} values and their temperature dependence.[15] The molecule has two pyridyl nitrogens attached to the metal ion in *trans* coordination as in $Mn(4NOPy)_2(hfac)_2$. However, the plane of the nitroxide groups make a relatively large dihedral angle of ca. 40° to the pyridine rings, causing a weak through-bond magnetic interaction between the metal ion and the unpaired electron of the nitroxide radicals. In addition, the nitroxide radical is situated close (O···O length of 2.74 Å) to another nitroxide radical of the adjacent complex molecule, leading to strong antiferromagnetic interaction. A similar mechanism is tentatively proposed for $Mn(3NOPy)_2(hfac)_2$, although a conclusive interpretation of the μ_{eff} value and its temperature dependence cannot be given until its molecular and crystal structure is determined to be similar to $Cu(3NOPy)_2(hfac)_2$.

C. 1:1 $Mn^{II}(hfac)_2$ Complexes with 3NOPy and 4NOPy. C-1. Possible Structures and X-ray crystal and Molecular Structure of 1:1 Complex a, $[Mn(4NOPy)(hfac)_2]_2$. Since the ligands 3- and 4NOPy are bis(monodentate) and capable of ligating at the nitrogen of the pyridine moiety and the oxygen of the nitroxide, there are a number of structural possibilities for 1:1 complexes. There are two kinds of monomers in which the Mn(II) ion is ligated either with N or O. Polymerization of these should lead in principle to head-to-tail, head-to-head/tail-to-tail, or irregular polymers. Cyclodimerization would give two macrocycles in which both Mn(II) ions are ligated with one N and one O with a formal center of symmetry or one Mn(II) ion is attached to two N's and the other to two O's with a formal plane of symmetry. There are a number of other possibilities for oligomerization.

The crystallographic and experimental parameters for the complex **a** are listed in Table 1. The 1:1 complex **a** has a cyclic dimer structure in which the oxygen of the nitroxide and the pyridyl nitrogen of one bis(monodentate) ligand are coordinated to different manganese ions in a *cis* configuration. As shown in Figure 5, the molecular structure has a center of symmetry. The dihedral angle between the pyridine ring and the nitroxide is about 33.5° and the distance between the two manganese ions in the dimer molecule is 8.498(4) Å. Selected bond lengths and angles for $[Mn(4NOPy)(hfac)_2]_2$ are given in Table 5. The molecular units are well separated from each other and the separation between the two nearest manganese ions belonging to two different units is 6.74 Å.

(15) Kitano, M.; Ishimaru, Y.; Inoue, K.; Koga, N.; Iwamura, H. unpublished results.

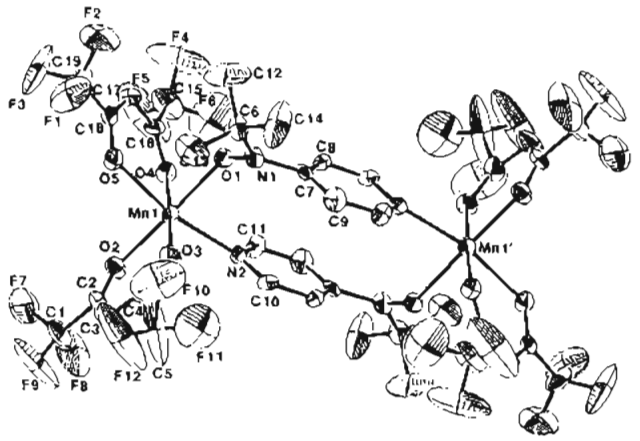

Figure 5. ORTEP view of $[Mn(4NOPy)(hfac)_2]_2$ (complex **a**) at 30% probability.

Table 5. Selected Bond Distances (Å) and Angles (deg) for $[Mn(4NOPy)(hfac)_2]_2$ (Complex **a**)[a]

	Bond Lengths (Å)		
Mn−Mn(1)	8.498(4)	Mn−O(4)	2.123(7)
Mn−O(1)	2.196(7)	Mn−O(5)	2.192(7)
Mn−O(2)	2.147(7)	Mn−N(2)	2.263(8)
Mn−O(3)	2.116(7)	O(1)−N(1)	1.299(9)
	Bond Angles (deg)		
O(1)−Mn−O(2)	176.3(3)	O(2)−Mn−N(2)	97.3(3)
O(1)−Mn−O(3)	94.5(3)	O(3)−Mn−O(4)	176.8(3)
O(1)−Mn−O(4)	88.0(3)	O(3)−Mn−O(5)	95.9(3)
O(1)−Mn−O(5)	84.7(3)	O(3)−Mn−N(2)	93.0(3)
O(1)−Mn−N(2)	85.5(3)	O(4)−Mn−O(5)	82.3(3)
O(2)−Mn−O(3)	84.1(3)	O(4)−Mn−N(2)	89.2(3)
O(2)−Mn−O(4)	93.3(3)	O(5)−Mn−N(2)	167.2(3)
O(2)−Mn−O(5)	92.7(3)		

[a] Standard deviations in the last significant digits are given in parentheses.

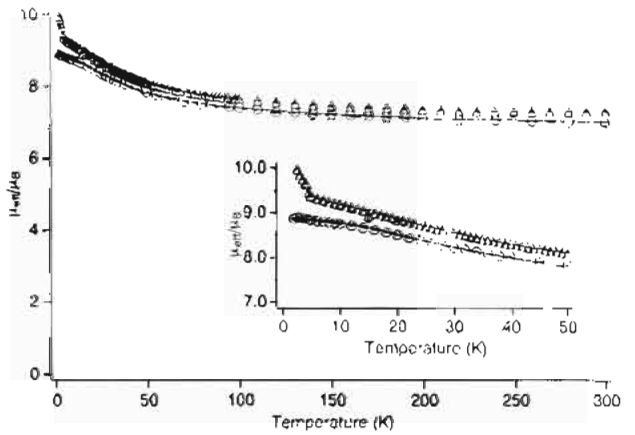

Figure 6. Temperature dependence of the effective magnetic moments μ_{eff} of 1:1 complexes $[Mn(4NOPy)(hfac)_2]$, complex **a** (○) and complex **b** (△). The inset shows the expanion of the μ_{eff} values below 50 K. Solid curves are theoretical ones calculated on the basis of eq 3 with the optimized parameters given in text.

C-2. Magnetic Properties of 1:1 Complexes a and b. The magnetic susceptibilities of microcrystalline samples of both 1:1 complexes were measured at 2−300 K at a constant field of 50 mT.

The μ_{eff} vs T plot for complex **a** is shown in Figure 6. The μ_{eff} value of 7.02 μ_B at 300 K is in good agreement with the theoretical spin-only value of $\mu_{eff} = 6.93\ \mu_B$ for two degenerate $S = {}^4/_2$ ($={}^5/_2 - {}^1/_2$) species with $g = 2$. As the temperature was decreased to 2 K, the μ_{eff}/μ_B value began to increase gradually and approached to a theoretical value of 8.94 for $S = 4$ at 2 K.

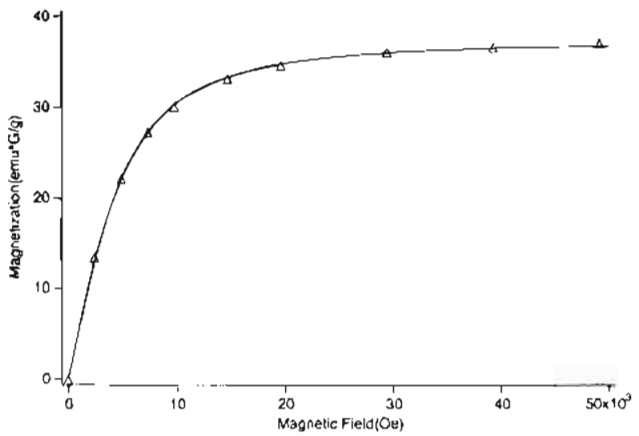

Figure 7. Field dependence of the magnetization of complex **b**, [Mn(4NOPy)(hfac)$_2$], at 1.8 K. The solid curve is a theoretical one calculated on the basis of the Brillouin function[18] with $S = 4.8$.

According to the molecular structure revealed by X-ray analysis, the cyclic dimer structure should be interpreted in terms of a cyclic array of four spins ${}^5/_2$, ${}^1/_2$, ${}^5/_2$, and ${}^1/_2$. The μ_{eff} data at 300 and 2 K seem to suggest that, since the exchange interaction between the Mn(II) ion and the directly attached nitroxide radical is considerably stronger and antiferromagnetic ($J/k_B = -100$ to -200 K),[16] the system may be regarded with good approximation as composed of two $S = {}^4/_2$ spins coupled weakly (by J) through two nonmagnetic head-to-tail couplers. The temperature dependence of μ_{eff} is then given by eq 3,[17] where all the symbols have their usual meaning. Fitting of eq

$$\mu_{eff}/\mu_B = \sqrt{g^2 \frac{84 + 6\exp\mathbf{B} + 30\exp\mathbf{C} + 180\exp\mathbf{D}}{7 + \exp\mathbf{A} + 3\exp\mathbf{B} + 5\exp\mathbf{C} + 9\exp\mathbf{D}}}$$

$$\mathbf{A} = \frac{-12J}{k_BT} \quad \mathbf{B} = \frac{-10J}{k_BT} \quad \mathbf{C} = \frac{-6J}{k_BT} \quad \mathbf{D} = \frac{8J}{k_BT} \quad (3)$$

3 to the observed μ_{eff} vs T plot of the dimeric Mn(II) complex by means of a least-squares method gave $J/k_B = +4.35 \pm 0.05$ K and $g = 1.970$. The calculated temperature dependence of μ_{eff}/μ_B is shown in Figure 6 as a solid curve.

The magnetic susceptibility for complex **b** measured under similar conditions showed a temperature dependent behavior similar to complex **a**. The $\mu_{eff} = 7.32\ \mu_B$ at 300 K was slightly higher than the one for complex **a**. As the temperature was lowered from 300 to 4.5 K, the μ_{eff} value increased gradually in a manner similar to complex **a** and then steeply below 4.5 K. The temperature dependence below 50 K is presented as an inset in Figure 6. The value at 17 K surpassed a theoretical value of $\mu_{eff} = 8.94\ \mu_B$ for the cyclic dimer structure with $S = 4$ such as complex **a**. In order to determine the effective spin quantum number in the low temperature region, the magnetization (M) for complex **b** was measured at 1.8 K on a Faraday balance. The saturation magnetization value M_s of 36 emu G g^{-1} is in good agreement with the $M_s = 35.2$ emu G g^{-1} calculated for a 1:1 complex for $S = {}^4/_2$. The M values obtained in the magnetic field range 0−5 T were fitted to the Brillouin function[18] with $J = S = 4.8$ as shown by the best fit curve represented by a solid line in Figure 7. The value is clearly higher than a ferromagnetically coupled dimer of two $S = {}^4/_2$'s, suggesting the occurrence of ferromagnetic interaction between the 1:1 units.

(16) Richardson, P. F.; Kreilick, R. W. *J. Phys. Chem.* **1978**, *82*, 1149. Dickman, M. H.; Porter, L. C.; Doedens, R. *J. Inorg. Chem.* **1986**, *25*, 2595. Caneschi, A.; Gatteschi, D.; Laugier, J.; Pardi, L.; Rey, P.; Zanchini, C. *Inorg. Chem.* **1988**, *27* 2027. Caneschi, A.; Gatteschi, D.; Sessoli, R.; Rey, P. *Acc. Chem. Res.* **1989**, *22*, 392.
(17) O'Connor, C. J. *Prog. Inorg. Chem.* **1981**, *29*, 203.

Scheme 1

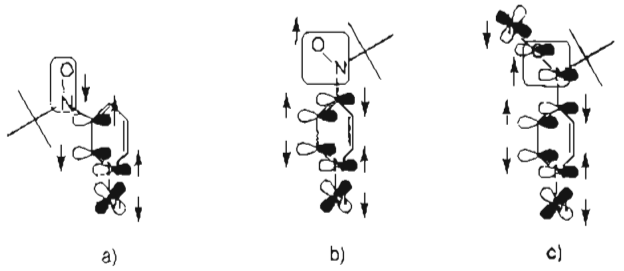

Although no direct structural information is available for complex **b**, the temperature dependence of the effective magnetic moment at temperatures below 4.5 K and the magnetization experiment strongly suggest that a part of complex **b** does not have a dimer structure such as complex **a** but exist as a higher oligomer.

D. Mechanism of the Exchange Interaction between Metals and Nitroxide Radicals. The chromium(III) ion in the porphyrin complexes has three unpaired electrons on the d_{xy}, d_{yz}, and d_{xz} orbitals each of which is a π magnetic orbital while the manganese(II) ion in the hfac complexes has both σ and π magnetic orbitals, two (d_{xz} and d_{yz}) of which will be able to overlap with the π orbital of the pyridine ring. In addition, hfs values, a_N and a_H, obtained in the EPR spectra of ligands 3- and 4NOPy suggest that the unpaired electrons of the nitroxide radical centers can delocalize onto the pyridine rings. Therefore, both spins on the metal ions and the radical centers are expected to interact magnetically through the π-conjugated systems and the sign of the exchange interaction can be explained by a spin polarization mechanism of the π-electrons. Ferro- and antiferromagnetic interactions between the metal ions and the NO radicals at 3 and 4 positions of the pyridine rings are schematically shown in Scheme 1a, b, respectively.

When the J value of $Mn(4NOPy)_2(hfac)_2$ was compared with that of a similar $Mn(hfac)_2$ complex with 2-(4-pyridyl)-4,4,5,5-tetramethylimidazolin-1-oxyl-3-oxide, $Mn(4NITPy)_2(hfac)_2$,[6] we note that the sign of the exchange interaction is opposite: negative for 4NOPy and positive for 4NITPy. The opposite sign of J could be explained by the different phase of the spin polarization of the π-electrons on the pyridine rings, as the imidazoline (NIT) has one extra carbon compared with *N-tert*-butyl nitroxide. The magnitude of the J value ($|J/k_B| = 12.4$ K) for 4NOPy is more than ten times larger than the one ($|J/k_B| = 0.75$ K)[6] for 4NITPy, showing that the delocalization of the π-spin from the *N-tert*-butyl nitroxide group to the pyridine ring is greater than in NITPy. This reduction in magnitude is caused by the fact that the singly occupied MO of NIT has a node at the 2-carbon between the two nitrogens in addition to the reduced planarity between the radical center and the pyridine ring in the complexes: 1.7° and 16.4° for $Mn(4NOPy)_2(hfac)_2$ and $Mn(4NITPy)_2(hfac)_2$, respectively.

Similarly, the observed ferromagnetic interaction between the two manganese ions in one unit of the 1:1 complex **a** can be explained as depicted in Scheme 1c. Previously,[19] we reported that the $Mn(hfac)_2$ complexes, $[Mn(3\text{- and }4NOIm)(hfac)_2]_2$, coordinated with a (1-imidazolyl)phenyl *tert*-butyl nitroxide in place of a pyridyl *tert*-butyl nitroxide had cyclic dimer structures similar to complex **a** and they showed similar regioselectivity in the sign of the exchange coupling between the two manganese ions. However the J value was 1 order of magnitude smaller than that of complex **a** (0.59 K for $[Mn(4NOIm)(hfac)_2]_2$ and 4.61 K for complex **a**), indicating that it would depend on the length of the π-bonds between the metal centers (the former is longer by the imidazole unit: 8.50 and 10.99 Å for complex **a** and $[Mn(4NOIm)(hfac)_2]_2$, respectively). Therefore, it is important for the design of the ligand molecule having a strong exchange interaction to shorten the distance between the ligating site and the radical center as much as possible.

When the J values for Cr(TPP)Cl and Cr(TAP)Cl complexes are compared, the exchange interaction was found to become slightly stronger by substitution of a hydrogen with a methoxy group in the *meso*-phenyl groups. Furthermore, by replacing hfac with acac in the $Mn(4NOPy)_2(hfac)_2$ complex, the J value was slightly decreased. It is worth noting from these observations that it is also possible to control the magnitude of the exchange interaction somewhat by the choice of the diamagnetic ligands.

Conclusions

The isomeric Cr(TPP)(3- and 4NOPy)Cl show a striking contrast in their intramolecular magnetic interactions; the d^3 electrons of chromium(III) porphyrins and the unpaired 2p electrons on the ligating 3- and 4NOPy have been found by EPR and SQUID measurements to interact ferro- and antiferromagnetically to give quintet and triplet ground states, respectively. It cannot be emphasized enough that the sign of the magnetic interaction can be controlled by the position of the nitroxide radical substituent on the pyridine ring as predicted by the spin polarization mechanism of the π-conjugated systems. Furthermore, in the $Mn(4NOPy)_2(hfac)_2$ complex, two nitroxide radicals interacted antiferromagnetically with the manganese ion, $J/k_B = -12.4 \pm 0.1$ K, through the π-electrons on the pyridyl rings in a *trans* position. The 1:1 complexes **a** obtained from $Mn(hfac)_2$ and 4NOPy has a cyclic *cis* dimer structure and a pair of $S = {}^4/_2$ units resulting from the strong antiferromagnetic interaction between the manganese ion ($S = {}^5/_2$) and the ligating nitroxide ($S = {}^1/_2$) interact ferromagnetically with $J/k_B = 4.35 \pm 0.05$ K. The magnetic properties of the complex **b** from $Mn(hfac)_2$ and 4NOPy suggest that it has an oligomeric structure (>dimer) and contains ferromagnetic interaction.

Acknowledgment. This work was supported by the Grant-in-Aid for Specially Promoted Research (No. 03102003) from the Ministry of Education, Science, and Culture of Japan.

Supplementary Material Available: Tables SI-SV and SVI-SX, listing experimental details, anisotropic displacement parameters, bond lengths, bond angles, and torsion angles for $Mn(4NOPy)_2(hfac)_2$ and $[Mn(4NOPy)(hfac)_2]_2$, respectively, Figures S1, showing the temperature dependences of μ_{eff} for Cr(TAP)(3- and 4NOPy)Cl, and Figure S2, showing an EPR spectrum of Cr(TAP)(4NOPy)Cl (28 pages). Ordering information is given on any current masthead page.

(18) $M = NgJ\mu_B BJ(x)$, where

$$B_J(x) = \frac{2J+1}{2J}\coth\frac{2J+1}{2J}x - \frac{1}{2J}\coth\frac{1}{2J}x$$

$$x = \frac{gJ\mu_B H}{k_B T}$$

(19) Ishimaru, Y.; Inoue, K.; Koga, N.; Iwamura, H. *Chem. Lett.* **1994**, 1693.